Proceedings of ISFOG 2025
5TH INTERNATIONAL SYMPOSIUM ON
FRONTIERS IN OFFSHORE GEOTECHNICS
Nantes, France | June 9-13 2025

ISBN 978-2-85782-758-0

Three dimensional finite element simulation of monopiles for offshore wind turbines using the HySand constitutive model

M. Saberi*
University of Oxford, Oxford, UK

L. E. J. Simonin
Université catholique de Louvain, Louvain-la-Neuve, Belgium (Formerly University of Oxford, UK)

G. T. Houlsby, and B. W. Byrne
University of Oxford, Oxford, UK

**miad.saberi@eng.ox.ac.uk*

ABSTRACT: The three-dimensional (3D) finite element (FE) method is routinely employed for designing and analysing monopile foundations for offshore wind turbines (OWT). However, reliable simulations require advanced soil constitutive models to capture accurately complex soil-foundation interactions under both monotonic and cyclic loading. This study investigates the application of the advanced sand model "HySand" to predict the behaviour of laterally loaded monopiles for OWT foundations using 3D FE simulations. HySand, an effective stress model based on hyperplasticity theory, simulates sand behaviour across various densities and confinement pressures under monotonic and cyclic, drained and undrained conditions. The model is first calibrated using laboratory soil test data, and its predictions are validated against these results. Following calibration, HySand is implemented into the ABAQUS FE code to evaluate its performance in simulating monopile responses. Monopiles of different geometries are modelled, and their force-displacement responses under varying soil densities and loading conditions, including monotonic and loading-unloading-reloading cycles, are analysed.

Keywords: Monopile; offshore wind turbine; HySand; constitutive modelling; finite element method

1 INTRODUCTION

Offshore wind energy is a cost-effective renewable source with significant global potential. Monopiles, large-diameter (4–8 m) open-ended steel piles with an embedded length-to-diameter (*L*/*D*) ratios of 3–8, are preferred foundation for offshore wind turbines (OWT) in shallow waters due to their simple fabrication and installation. With increasing turbine sizes, monopiles up to 10 m are being considered (Byrne *et al*. 2015, 2020; Murphy *et al*. 2018). As foundation costs are major expenses, optimizing OWT design is essential and understanding monopile behavior under lateral loads from wind and waves is key to efficient geotechnical design.

Since the development of OWTs, various methods have been introduced to analyse laterally loaded monopiles, mostly using one-dimensional (1D) Winkler models with nonlinear springs. The stiffness of these springs is based on *p*-*y* curves, which link the lateral load (*p*) to lateral displacement (*y*). Early versions of these curves developed by Matlock (1970) and Reese *et al*. (1974) are still commonly used in design standards. However, these curves were designed for long, flexible piles with a length-to-diameter (*L*/*D*) ratio above 10, which is higher than values typically used for monopiles. Recently, new approaches have been suggested to improve 1D modelling for monopiles under lateral loads. Among these, the PISA design model (Burd *et al*. 2020, Byrne *et al*. 2020) has been adopted by the industry for monotonic conditions. Macro-element approaches (0D models), which encapsulate the entire soil-pile response in a single model, have also proven effective and efficient (Houlsby *et al*. 2017, Abadie *et al*. 2019). The most advanced method, however, is 3D FE modelling, which is widely used in research and industry to study complex soil-pile interactions. In these models, the key challenge is accurately representing the nonlinear soil behaviour and the soil-pile interaction, which are expressed mainly by soil constitutive models. In recent years, several 3D FE studies have investigated laterally loaded monopiles embedded in sand (Achmus *et al*. 2019, Ma *et al*. 2017, Murphy *et al*. 2018, Kementzetzidis *et al*. 2019, Staubach and Wichtmann 2020, Taborda *et al*. 2020, Liu *et al.* 2022), utilizing elasto-plastic soil constitutive models. However, few studies have used advanced soil constitutive models, essential for accurately capturing complex soil

behaviour under loading. A major challenge remains in developing and implementing a sophisticated yet efficient constitutive model for FE codes, that can accurately simulate sandy soil response in monopile foundations under various loading conditions.

This study presents, for the first time, the application of the advanced constitutive model "HySand", based on the hyperplasticity framework, for laterally loaded OWT monopiles. Model parameters are calibrated using available soil triaxial test data, and the calibrated model is then utilized in 3D FE simulations of monopiles subjected to lateral loads. Two medium and large-scale monopiles in sands with varying densities are simulated to study their responses to large lateral displacements and loading-unloading-reloading cycles under both displacement and load-controlled conditions.

2 HYSAND CONSTITUTIVE MODEL

HySand is an effective stress constitutive model, formulated within the framework of hyperplasticity theory and utilizing multiple yield surfaces. Hyperplasticity is a plasticity theory based on thermodynamic principles and has its roots in the work of Ziegler (1977). A comprehensive presentation of hyperplasticity can be found in Houlsby and Puzrin (2006). In this approach, the entire constitutive behaviour is derived from two scalar potentials. For HySand, these are the Gibbs energy function (g) and the yield surfaces (y). The Gibbs energy function represents the stored energy in the system and is defined in terms of stresses (the effective mean stress p, and deviatoric stress q) and internal variables (the volumetric plastic strain $\alpha_p^{(n)} + \alpha_{pc}^{(n)}$, and shear plastic strain $\alpha_q^{(n)}$, linked to the n^{th} yield surface).

HySand can simulate sand behaviour under varying densities and confinement pressures. It includes realistic modelling of the effects of pressure and density on both stiffness and dilative response. It can simulate both monotonic and cyclic drained and undrained conditions using a single set of model parameters. For detailed formulations and discussions of the model in both triaxial and generalized stress spaces, see Simonin (2023). In this study, for completeness, only the two scalar potentials, the Gibbs energy function and the yield surface, in triaxial space are presented in Table 1.

3 MODEL CALIBRATION

HySand uses 14 input parameters calibrated from monotonic and cyclic drained and undrained triaxial tests (detailed in Simonin 2023) and captures behaviours with a single set of parameters. This study employs Karlsruhe sand, with parameter calibration based on triaxial test data from Wichtmann and Triantafyllidis (2016). Table 2 presents the calibrated parameters, and Figures 1 and 2 compare the model predictions with laboratory tests for loose and dense sand under monotonic drained and undrained conditions. The parameter selection represents a compromise, based on a much larger database of tests than the four shown here. It is evident that there is a good agreement between the test data and the model predictions. In this study, the initial specific volume $v_0 = 1 + e_0$, where e_0 is the initial void ratio, indicates initial soil density.

Table 1. Triaxial formulation of HySand constitutive model

Gibbs energy function (g):

$$g = -\frac{p_r}{k_r(1-m)(2-m)}\left(\frac{p_0}{p_r}\right)^{2-m} - q\frac{1}{N}\sum_{n=1}^{N}\alpha_q^{(n)} - p\frac{1}{N}\sum_{n=1}^{N}(\alpha_p^{(n)} + \alpha_{pc}^{(n)}) \quad (1)$$

$$p_0^2 = p^2 + \frac{k_r(1-m)}{3g_r}\,q^2 \quad (2)$$

Yield functions (y):

$$y^{(n)} = \frac{\left(N\chi_q^{(n)} - h_n\left(p, q, \alpha_q^{(n)}\right) - a\beta^{(n)}N\chi_p^{(n)} + A(1-|a|)\chi_a\right)^2}{4\left(\frac{n}{N}\mu\right)^2\left(p + \frac{2}{3}q\right)\left(p - \frac{q}{3}\right)} + \left(\frac{N\chi_{pc}^{(n)}}{p_c^{(n)}}\right)^r - 1 \quad (3)$$

Description:

- N: number of yield surfaces
- p_r=*100 kPa* reference pressure
- χ: generalised stresses
- α: internal variables
- k_r, g_r: dimensionless elastic moduli
- m: non-linear elasticity pressure index
- h_n: hardening function
- p_c: consolidation pressure
- a: internal anisotropy scalar
- β: dilation ratio
- A: anisotropy development rate
- μ: friction ratio

* The 14 model input parameters and the full details of the model are discussed in Simonin (2023).

Table 2. HySand input parameters

Parameter	k_r	g_r	m	φ_c (°)	β_{max}	B	Γ
Value	493	417	0.73	34	1.09	2.054	1.97
1	**Δ**	**λ_B**	**λ_Δ**	**A_{max}**	**h_0**	**b**	**r**
Value	1.677	0.0059	0.0025	34.3	1216	3	0.22

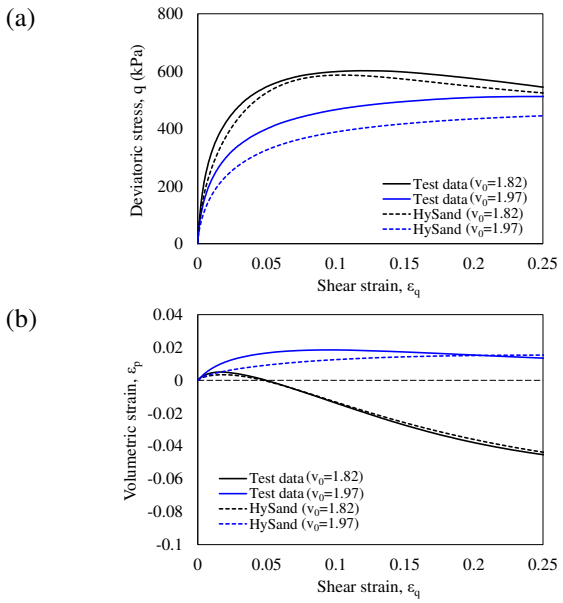

Figure 1. Comparison of HySand simulations with drained test data, (a) q-ε_q, and (b) ε_p-ε_q.

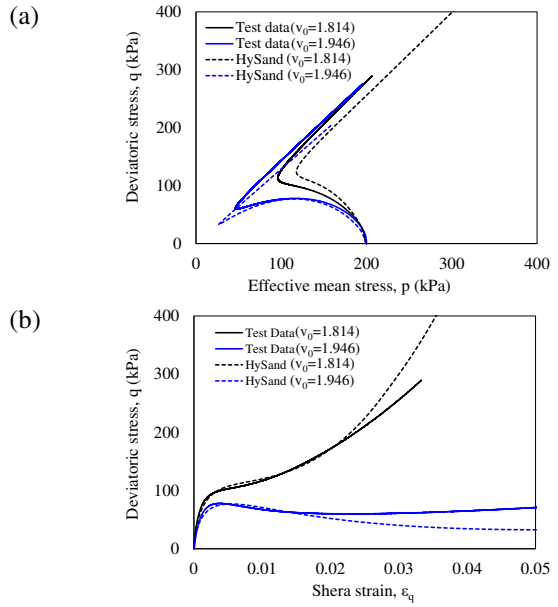

Figure 2. Comparison of HySand simulations with undrained test data, (a) q-p, and (b) ε_p-ε_q.

4 MONOPILE FE SIMULATION

This section examines the application of HySand in FE simulations of laterally loaded monopiles. HySand was implemented in the general-purpose FE code ABAQUS (Dassault Systemes 2021) through a UMAT user subroutine. Two monopiles, one medium-scale and one large-scale, were simulated. The monopile dimensions, including diameter (D), embedment length (L), loading height (h), and wall thickness (t), are summarized in Table 3. Both monopiles have the same low L/D and h/D ratios of 3 and 4, respectively, to better assess scaling effects. Figure 3 shows the FE model and simulated geometry for the medium-scale pile as a representative case.

In the FE models, the soil was simulated by solid elements, and the monopile was modelled using shell elements. To minimize boundary effects, the model boundaries were extended more than 16D from the pile centre. The soil around the pile was assumed to be saturated, and the simulations were performed under drained conditions. The HySand input parameters, calibrated in section 3, were used for two different densities: one dilative with $v_0 = 1.82$ and one contractive with $v_0 = 1.97$, capturing both dilative and contractive soil behaviour effects on monopile capacity. As shown in Figure 3, the load was applied at the pile head, and under monotonic conditions, loading continued until reaching a pile displacement of 0.2D at the ground surface. The coefficient of earth pressure at rest (K_0) was set to 1.0, and a 10 kPa surcharge was applied to the ground surface to ensure convergence of the analysis at low stress levels. The FE models have been validated against field data but these results are commercially confidential at present.

Table 3. Monopile dimensions in FE simulations

Pile size	D (m)	L (m)	h (m)	t (m)	h/D	L/D	D/t
Medium	1.22	3.66	4.88	13	4	3	~94
Large	8	24	32	85	4	3	~94

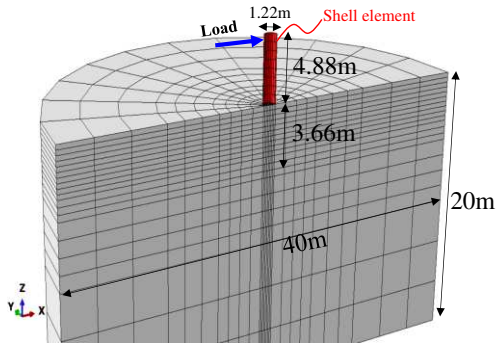

Figure 3. FE model for medium-scale monopile

5 NUMERICAL RESULTS

5.1 Monotonic Loading

This section presents numerical predictions for medium-scale (Figure 4a) and large-scale (Figure 4b) monopiles under lateral monotonic loading. The

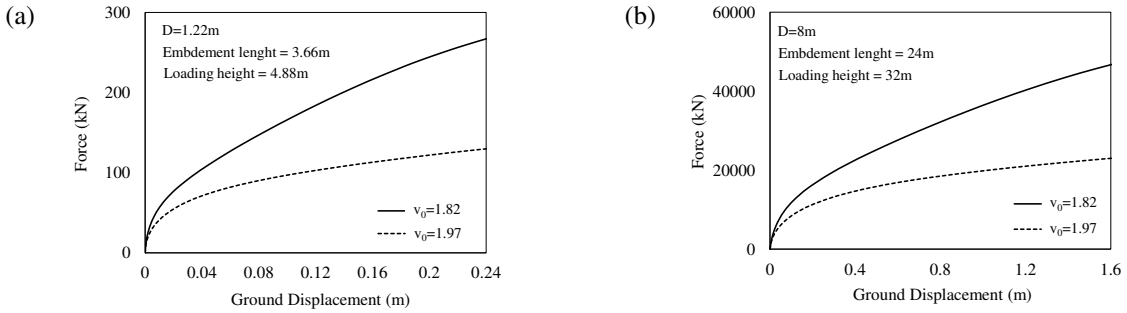

Figure 4. Monopile response predictions under monotonic loading, (a) medium-scale pile, and (b) large-scale pile.

force at the monopile head is plotted against ground level displacement for both dense (v_0 = 1.82) and loose (v_0 = 1.97) sands. The model successfully simulates large displacements of up to 0.2D at the ground surface, double the 0.1D commonly used in design. Figure 4 also shows that the pile in dense sand exhibits much higher resistance than in loose sand, and the force stabilizes more slowly in dense sand. Additionally, the large-scale pile demonstrates significantly greater capacity in both soil types compared to the medium-scale pile, as expected.

5.2 Loading-Unloading-Reloading

This section demonstrates HySand's ability to simulate the loading-unloading-reloading behaviour of monopiles with various amplitudes in dense and loose sand. To illustrate this, a single loop as well as two cycles are presented. Three types of loading loops were considered: 1-way, 2-way, and partial 2-way. Figure 5 and 6 present FE simulations of the force-displacement behaviours of medium and large monopiles in dense and loose sands under 2-way and partial 2-way loading. The model effectively captures complex behaviours during loading-unloading-reloading cycles, including hardening in the 2-way loop (Figure 5a-b, and 6a-b), and predicts well the monopile backbone curve after an unloading-reloading loop (Figure 5c-d, and 6c-d).

The HySand model implemented in the FE code effectively captures the ratcheting behaviour of monopiles under one-way loading, where lateral deformation accumulates with cyclic loading. To demonstrate this, the response of a medium-scale monopile was simulated under a few one-way cycles in dense and loose sand (Figure 7). The results show the model ability to effectively capture the deformation accumulation. This ratcheting arises naturally from cycle-by-cycle modeling and is influenced by parameter selection.

To analyse better monopile behaviour across different sizes, the force-displacement relationships are presented in a non-dimensional form. This study plots the responses of both medium and large-scale monopiles on the same graph as $H/\gamma' L^2 D$ versus

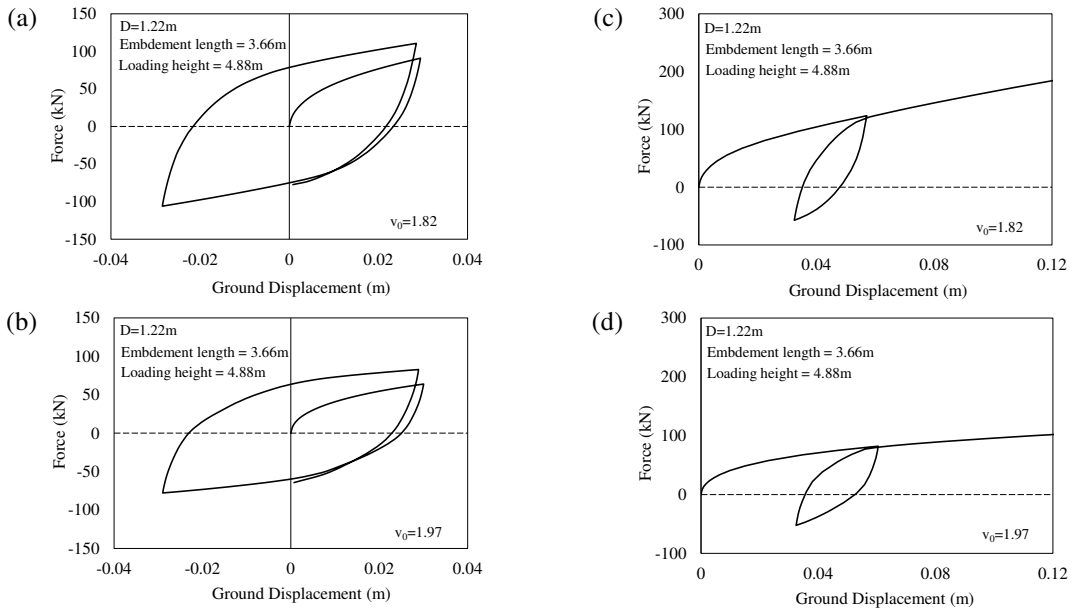

Figure 5. FE predictions for medium-scale monopile, (a) 2-way loading with v_0 = 1.82, (b) 2-way loading with v_0 = 1.97, (c) partial 2-way loading with v_0 = 1.82, and (d) partial 2-way loading with v_0 = 1.97.

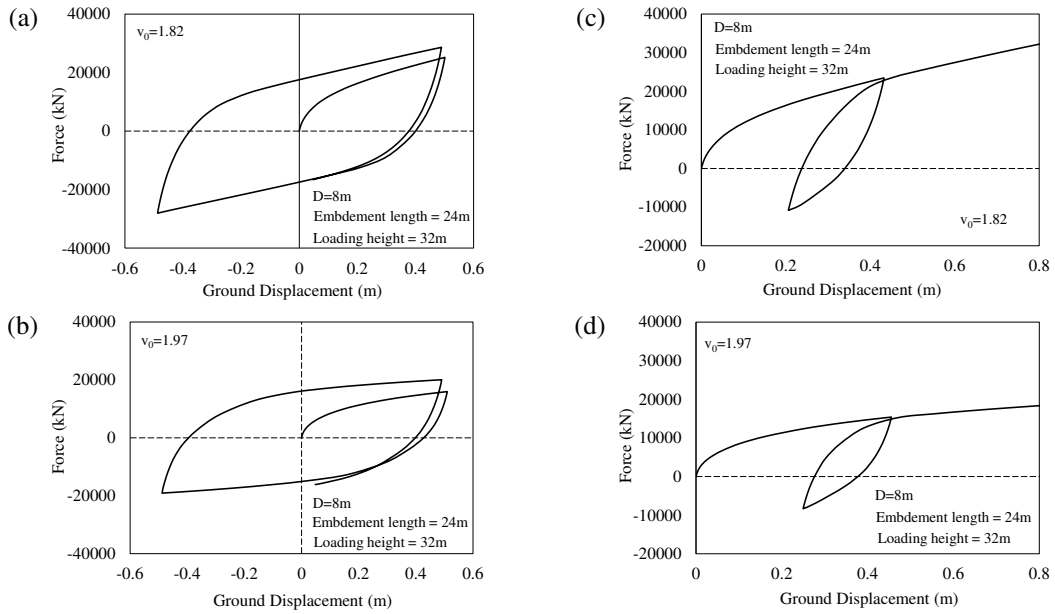

Figure 6. FE predictions for large-scale monopile, (a) 2-way loading with $v_0 = 1.82$, (b) 2-way loading with $v_0 = 1.97$, (c) partial 2-way loading with $v_0 = 1.82$, and (d) partial 2-way loading with $v_0 = 1.97$.

$\frac{v}{D}\sqrt{p_a/\gamma' L}$, where H is force, γ' is effective unit weight, L is embedment length, D is diameter, v is displacement, and p_a is a reference pressure (100 kPa). Figure 8 shows the scaled force-displacement response for two-way loading in dense (Figure 8a) and loose sand (Figure 8b) in non-dimensional form. As can be seen, the predicted 3D FE responses of medium and large-scale monopiles match closely in the non-dimensional plots. However, the larger pile shows a slightly weaker response in dimensionless terms, because of the reduction in frictional capacity with stress level (at the same density).

CONCLUSION

In this study, the advanced sand constitutive model "HySand," based on hyperplasticity theory, was implemented in the general-purpose FE code ABAQUS to predict the lateral response of OWT monopiles. The model was first calibrated using triaxial test data (drained and undrained) before being employed in FE simulations. Two monopiles, one medium-scale and one large-scale, were simulated in both dense and loose sands, capturing dilative and contractive behaviours. The simulations demonstrate HySand's capability to predict nonlinear monopile

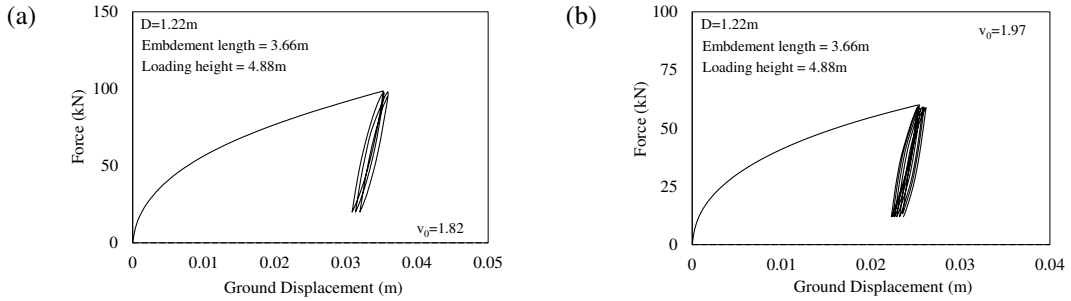

Figure 7. Medium-scale monopile response predictions under few cycles for, (a) dense sand and (b) loose sand.

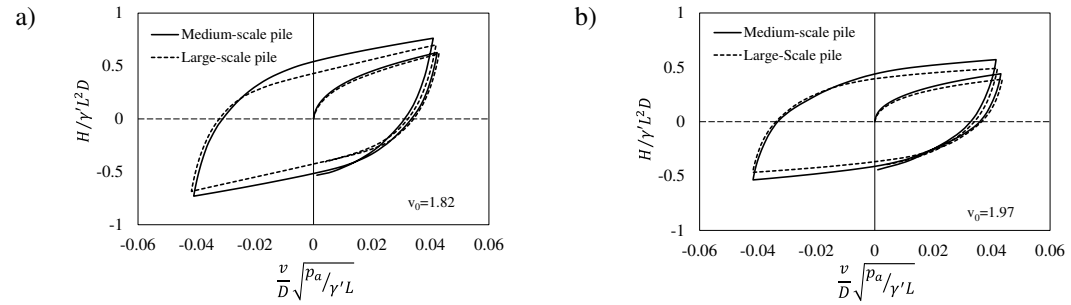

Figure 8. Normalized response of medium and large-scale monopiles in, (a) dense sand and (b) loose sand.

responses under monotonic and loading-unloading-reloading cycles across various sand densities and monopile sizes. The model effectively captures ratcheting behaviour and scaled monopile responses. It also successfully simulated lateral displacements of up to 0.1*D* and 0.2*D* at ground level, aligning with common design criteria.

AUTHOR CONTRIBUTION STATEMENT

M. Saberi: Conceptualization, Formal analysis, Software, Visualization, Validation, Writing–original draft. **L. E. J. Simonin:** Conceptualization, Formal analysis, Software, Validation, Writing-review & editing. **G. T. Houlsby**: Supervision, Conceptualization, Software, Validation, Writing–review & editing. **B. W. Byrne:** Supervision, Conceptualization, Funding acquisition, Resources, Writing–review & editing.

ACKNOWLEDGEMENTS

The authors gratefully acknowledge the financial support provided by Ørsted for the successful completion of this research project.

REFERENCES

Abadie, C.N., Houlsby, G.T., and Byrne, B.W. (2019). A method for calibration of the Hyperplastic Accelerated Ratcheting Model (HARM). *Computers and Geotechnics*, 112, pp. 370–385. https://doi.org/10.1016/j.compgeo.2019.04.017

Achmus, M., Thieken, K., Saathoff, J.E., Terceros, M., and Albiker, J. (2019). Un- and reloading stiffness of monopile foundations in sand. *Appl. Ocean Res.*, 84, pp. 62–73. https://doi.org/10.1016/j.apor.2019.01.001

Burd, H.J., Taborda, D.M.G., Zdravkovic, L., Abadie, C.N., Byrne, B.W., Houlsby, G.T., Gavin, K.G., Igoe, D.J.P., Jardine, R.J., Martin, C.M., McAdam, R.A., Pedro, A.M.G., and Potts, D.M. (2020). PISA design model for monopiles for offshore wind turbines: Application to a marine sand. *Géotechnique*, 70(11), pp. 1048–1066. https://doi:10.1680/jgeot.18.P.277

Byrne, B.W., Houlsby, G.T., Burd, H.J., Gavin, K.G., Igoe, D.J.P., Jardine, R.J., Martin, C.M., McAdam, R.A., Potts, D.M., Taborda, D.M.G., and Zdravkovic, L. (2020). PISA design model for monopiles for offshore wind turbines: Application to a stiff glacial clay till. *Géotechnique*, 70(11): 1030–1047. https://doi.org/10.1680/jgeot.18.P.255

Byrne, B.W., McAdam, R., Burd, H.J., Houlsby, G.T., Martin, C.M., Zdravković, L., Taborda, D.M.G., Potts, D.M., Jardine, R.J., Sideri, M., Schroeder, F.C., Gavin, K., Doherty, P., Igoe, D., Muirwood, A., Kallehave, D., and Skov Gretlund, J. (2015). New design methods for large diameter piles under lateral loading for offshore wind applications. In: *Frontiers in Offshore Geotechnics III,* CRC Press, London, UK, pp. 705–710. https://doi.org/10.1201/b18442

Dassault Systemes (2021). *Abaqus Documentation*.

Houlsby, G.T., Abadie, C.N., Beuckelaers, W.J.A.P., and Byrne, B.W. (2017). A model for nonlinear hysteretic and ratcheting behaviour. *International Journal of Solids and Structures*, 120, pp. 67–80. https://doi.org/10.1016/j.ijsolstr.2017.04.031

Houlsby, G.T., and Puzrin, A.M. (2006). *Principles of Hyperplasticity: An Approach to Plasticity Theory Based on Thermodynamic Principles*. Springer, London.

Kementzetzidis, E., Corciulo, S., Versteijlen, W.G., and Pisanò, F. (2019). Geotechnical aspects of offshore wind turbine dynamics from 3D non-linear soil-structure simulations. *Soil Dynamics and Earthquake Eng.*, 120, pp. 181–199. https://doi.org/10.1016/j.soildyn.2019.01.037

Liu, H., Kementzetzidis, E., Abell, J.A., and Pisanò, F. (2022). From cyclic sand ratcheting to tilt accumulation of offshore monopiles: 3D FE modelling using SANISAND-MS. *Géotechnique*, 72(9):753–768. https://doi.org/10.1680/jgeot.20.P.029

Ma, H., Yang, J., and Chen, L. (2017). Numerical analysis of the long-term performance of offshore wind turbines supported by monopiles. *Ocean Eng.*, 136, pp. 94–105. https://doi.org/10.1016/j.oceaneng.2017.03.019

Matlock, H. (1970). Correlation for Design of Laterally Loaded Piles in Soft Clay. In *Offshore Technology Conference*. Houston, Texas, USA.

Murphy, G., Igoe, D., Doherty, P., and Gavin, K. (2018). 3D FEM approach for laterally loaded monopile design. *Computers and Geotechnics*, 100, pp. 76–83. https://doi.org/10.1016/j.compgeo.2018.03.013

Reese, L.C., Cox, W.R., and Koop, F.D. (1974). Analysis of Laterally Loaded Piles in Sand. In *Offshore Technology Conference*. Houston, Texas, USA.

Simonin, L. (2023). *Development of an effective stress model for sand under cyclic loading in the hyperplastic framework*. DPhil thesis, University of Oxford, UK.

Staubach, P., and Wichtmann, T. (2020). Long-term deformations of monopile foundations for offshore wind turbines studied with a high-cycle accumulation model. *Computers and Geotechnics*, 124. https://doi.org/10.1016/j.compgeo.2020.103553

Taborda, D.M.G., Zdravkovic, L. et al. (2020). Finite-element modelling of laterally loaded piles in a dense marine sand at Dunkirk. *Géotechnique* 70(11), pp. 1014–1029. https://doi.org/10.1680/jgeot.18.PISA.006

Wichtmann, T., and Triantafyllidis, T. (2016). An experimental database for the development, calibration and verification of constitutive models for sand with focus to cyclic loading: part II—tests with strain cycles and combined loading. *Acta Geotechnica*, 11(4), pp. 763–774. https://doi.org/10.1007/s11440-015-0412-x

Ziegler, H. (1977). *An Introduction to Thermomechanics*. North Holland, Amsterdam.